

Heat Capacity and Thermodynamic Properties of α -Beryllium Nitride, Be_3N_2 , from 20 to 315 K*

George T. Furukawa and Martin L. Reilly

Institute for Basic Standards, National Bureau of Standards, Washington, D.C. 20234

(May 27, 1970)

The heat capacity of α -beryllium nitride, Be_3N_2 , was determined from 20 to 315 K and the thermodynamic properties calculated from 0 to 315 K. The entropy at 298.15 K was found to be 34.4 ± 0.3 J/K·mol (8.23 ± 0.08 cal/K·mol). The precision using a calorimeter of a new design is shown to be ± 0.01 percent over most of the temperature range of the measurements.

Key words: α -beryllium nitride; calorimeter; entropy; heat capacity; specific heat; thermodynamic properties.

1. Introduction

The results of heat-capacity measurements of α -beryllium nitride, Be_3N_2 , presented between 20 and 315 K in this paper have been obtained in connection with a research program at the National Bureau of Standards to provide thermodynamic data on light-element compounds. In connection with this program, the high-temperature enthalpy measurements have previously been reported by Douglas and Payne [1]¹. Earlier, Satoh [2] reported relative enthalpy measurements at three temperatures in the range 273 to 773 K on a sample of 98.13 weight percent purity, the impurities being 0.78, 0.87, and 0.22 percent BeO , Fe_2O_3 , and SiO_2 , respectively. Recently Justice [3] reported measurements in the range 25 to 310 K on a sample of 96.7 weight percent purity.

2. Apparatus and Method

The low-temperature heat-capacity measurements were made from about 20 to 315 K in an adiabatic calorimeter of a design similar in principle to that described previously [4]. Many design changes have been incorporated in calorimeters that have since been constructed. Although results of heat-capacity measurements obtained with them have been published, e.g., references [5, 6, 7, 8], no detailed descriptions of the calorimeters have been reported at their successive stages of development. Changes have been made to facilitate the assembly of the calorimeter, to achieve better temperature control of the electrical

leads, and to improve the quality of automatic control of the adiabatic shield. In the design of the new calorimeter used for the measurements on beryllium nitride, a provision was made for the calibration, when ever required, of the resistance thermometer attached to the calorimeter vessel during the heat-capacity measurements. Thus, samples of a wide range of sizes and shapes can be investigated in the calorimeter provided that a resistance thermometer and a thermocouple can be attached in good thermal contact with the sample or the sample "holder." Although the new calorimeter is considered already "obsolete" in some respects, its description is given in this paper for purposes of a record of a stage in calorimeter development.

Figure 1 shows a schematic drawing of the calorimeter. Briefly, the double-walled sample vessel containing a resistance thermometer and heater is suspended in a vacuum space by means of a nylon cord. The vessel is thermally shielded from radiation by a thin gold-plated copper "jacket" maintained at the same temperature as the same vessel. The heat conduction along the electrical lead wires to the sample vessel is controlled separately at the "thermometer-heater lead control," which also contains the reference platinum resistance thermometer. The thermometer in the sample vessel is calibrated against the reference thermometer in the "thermometer-heater lead control," which is maintained at the same temperature as the sample vessel. For the measurements with beryllium nitride, on which the performance of the calorimeter was tested, a calibrated platinum resistance thermometer was incorporated in the sample vessel to test the "calibration method." The results of the "calibration" are given in section 2.5.1.

The calorimeter system was cooled by immersing in a suitable refrigerant as described previously [4] and shown schematically in figure 1.

*This work was supported by the Advanced Research Projects Agency, Department of Defense, under Order No. 20 and by the Air Force Office of Scientific Research, Office of Aerospace Research, United States Air Force under AFOSR Contract No. ISSA 68-0004.

¹ Figures in brackets indicate the literature references at the end of this paper.

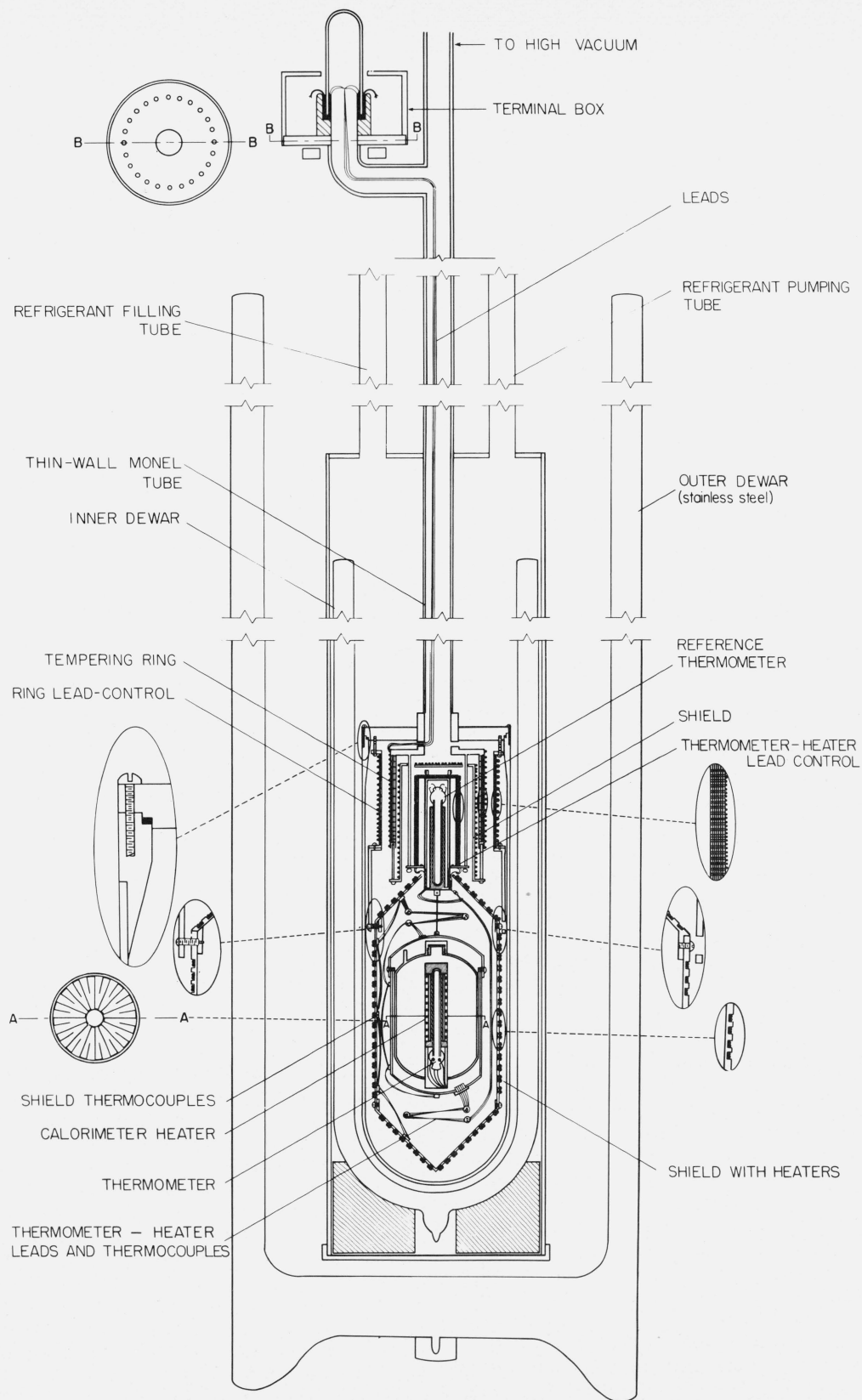


FIGURE 1. Schematic drawing of the calorimeter assembly with dewar arrangements.

The inner dewar system is employed with the following refrigerants: liquid hydrogen, pumped liquid or solid hydrogen, or pumped liquid or solid nitrogen.

Details of the calorimeter design and construction are described in the following sections. *Reference to trade names is made only for identification and simplification of description and does not imply in any way the endorsement of the products by the National Bureau of Standards.*

2.1. Cement

The adhesive used for cementing the wires and thermocouple assembly for thermal contact was exclusively Glyptal lacquer at full strength or diluted with xylene. After application, the lacquer was air dried at 130 °C for 6 hr.

2.2. Wires

2.2.1. Electric Lead Wires

The electric lead wires were all 0.160-mm-diam (AWG No. 34) copper, insulated with a heavy coating of Formvar enamel and double silk wrap. Before using the wire, a dilute solution of lacquer (1 part lacquer to 5 parts xylene) was applied to improve the bonding and abrasion resistance of the silk insulation. The outside diameter of the insulated wire was about 0.280 mm.

2.2.2. Thermocouple Wires

The thermocouple wires (0.127 mm diam) were constantan and Chromel-P insulated with double silk wrap. A dilute solution of lacquer was also applied to the wires to improve the bonding and abrasion resistance of the silk insulation.

Three methods were used to attach the thermocouples for sensing temperatures. In the first method, the two thermocouple wires were soldered to thin copper disks (5 mm diam \times 0.051 mm thick) with a "clearance hole" at the center for a screw. The disks in turn were attached to temperature-sensing points ("threaded holes") with screws using thin mica disks (0.013 mm thick) for electrical insulation. A thin layer of lacquer was applied between the surfaces to improve the thermal contact. This method was used to sense the temperature on the "thermometer-heater lead control" and its shield, "ring lead control," and "tempering ring."

In the second method, the two thermocouple wires were soldered to thin copper strips (3 mm wide \times 20 mm long \times 0.051 mm thick). The strips were in turn cemented with lacquer to temperature-sensing points using thin mica sheets (0.013 mm thick) for electrical insulation. This method was used on the "thermometer-heater lead control" to sense its temperature relative to the sample vessel. The strips were arranged parallel to the axis and around the cylindrical surface of the "thermometer-heater lead control" and a double silk insulated copper wire (0.079 mm diam) was wound tightly over the strips to improve the thermal contact and mechanical strength. A dilute solution of lacquer (1 part lacquer to 3 parts xylene) was applied over the assembly.



FIGURE 2. Calorimeter assembly with vacuum can and sample vessel removed.

In the third method, the two thermocouple wires were soldered together and placed between two mica sheets (0.025 mm thick); then a gold-plated copper sheath (0.20 mm thick) was crimped over them. A thin layer of lacquer was applied between the layers before crimping the copper sheath. These sheathed thermocouples were used with rather broad "M-shaped" holders silver soldered on the radiation shield and on the sample vessel. (Figs. 2 and 3 show the sheathed thermocouples both before and after being wedged into the tightly sprung M-shaped holders). A very thin layer of stopcock grease was applied to the sheathed thermocouples used on the sample vessel to improve the thermal contact. The total mass of grease was less than 0.1 mg.

2.2.3. Heater Wires

Approximately 75 percent Ni-20 percent Cr alloy was used for the "calorimeter heater" because of its small change in resistance (less than 1 percent) over the temperature range of measurements [10]. The insulation on the wire was double glass-fiber wrap with silicone enamel as the binder. The heater resistance was 100 Ω .

The heater wires (0.160 mm diam) used for temperature control on the adiabatic shields and "electrical lead controls" were copper-nickel alloys insulated with double glass-fiber wrap with silicone enamel as binder. The outside diameter of the insulated wires

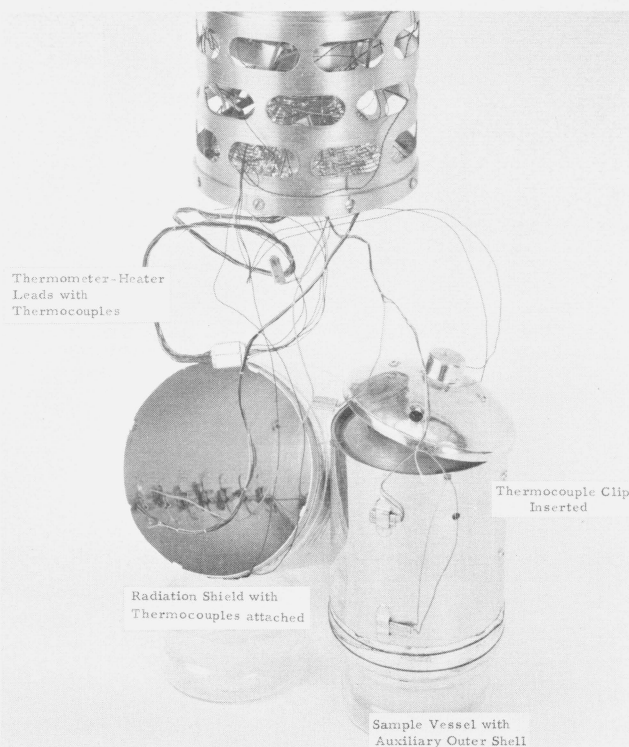


FIGURE 3. Interior view of radiation shield for sample vessel and sample vessel with auxiliary outer shell.

was about 0.340 mm. Alloy wires of different Cu-Ni compositions were selected to yield a total resistance of about 200 Ω for each of the control heaters.

2.3. Adiabatic Shields

The calorimeter sample vessel was "adiabatically shielded" by a combination of a radiation shield, a high vacuum (10^{-5} torr or better) to minimize gaseous heat conduction, and temperature control of electrical leads to the sample vessel. The temperature of the radiation shield surrounding the sample vessel was controlled independently from that of the electrical leads to the vessel. The details of the design used in the radiation shields and for the control of electrical lead temperature will be given separately.

2.3.1. Temperature Control and Tempering of Electrical Lead Wires

a. Temperature control of electrical lead wires. All electrical leads entered the calorimeter through the Apiezon W wax seal at the terminal box and traversed the length of the high vacuum pump-out tube. (See fig. 1.) The leads were then attached to the "tempering ring" and later attached to the "ring lead-control." After the "ring lead-control" the lead wires were attached to the "thermometer-heater lead-control." before going to the sample vessel. At each of the above locations some of the wires branched out to thermocouples and to heaters.

At the "tempering ring," the electrical leads were

brought to the temperature of the refrigerant in which the calorimeter was immersed. At the "ring lead-control," the temperature of the leads was raised close to that of the "thermometer-heater lead control." At the "thermometer-heater lead control" the leads were maintained at the same temperature as that of the sample vessel.

b. Tempering of electric lead wires. The copper lead wires (0.280 mm diam including insulation) were tempered by individually cementing them with lacquer (full strength) into separate, tightly fitting grooves (0.254 mm wide \times 0.254 mm deep) machined "along" the cylindrical copper surface parallel to its axis.² The heater wires were tightly wound (helic ally) over the copper wires and cemented. The "ring lead-control" and "thermometer-heater lead control" were wired in this manner. (See insert of fig. 1.) On the "tempering ring," where heating was not needed, insulated copper wire was wound over the lead wires to improve the thermal contact and mechanical strength. A dilute solution of lacquer (1 part lacquer to 3 parts xylene) was applied over the wires.

2.3.2. Radiation Shields

a. Shield for the calorimeter vessel. This radiation shield was essentially a thin copper shell of 0.810 mm thickness consisting of three sections, a cylinder and two end cones (90°). Screws held the two cones to the cylinder. A thin film of grease was used between the surfaces that were in contact. For the heater wire, an evenly spaced groove (0.620 mm wide \times 0.310 mm deep) was machined helically on the cylinder and "spirally" on the cones. The distribution of the heater wire grooves was made very nearly the same over the entire shield surface to yield even heating. The M-shaped thermocouple holders were silver-soldered on the inner surface of the shield. The shield was gold-plated.

A pair of heater wires was wound into the tightly fitting groove of the shield. The procedure for winding the heater wire was first to paint the groove with lacquer (full strength) and to press the wire pair into the groove before the lacquer dried. In the process the excess lacquer was pushed out. Additional lacquer (1 part lacquer to 3 parts xylene) was applied over the wire and copper shield. The heater wires on the cones and on the cylinder were connected in series.

The sheathed thermocouples for sensing the shield temperature relative to that of the sample vessel surface were inserted into the tightly fitting M-shaped holders. A thin layer of lacquer was applied to these surfaces to improve the thermal contact. (See figs. 1 and 3). Thermocouples were attached at five locations on the radiation shield: three on the cylindrical portion and one on each conical ends. The corresponding four locations on the sample vessel were: one at each end and two on the side.

² A blunt tool was run through the grooves to eliminate any machining "burrs" and to provide a very smooth surface for the insulated wires. To date after six years of use, no wire has become grounded or "shorted" to another one.

2.4. Sample Vessel

The cross-sectional views of the sample vessel are shown in figure 1. The vessel was essentially all copper construction with outer surfaces gold plated. The parts of the vessel were assembled with "silver solder." The inner container surface was covered with a thin layer of tin which served also to "solder" the vanes in place. The auxiliary outer thin copper shell served to achieve more reproducible surface temperatures between the vessel plus sample and empty vessel measurements. The thermometer and calorimeter heater were centrally located in a re-entrant well of the inner vessel.

The thermocouple junctions (six) for sensing the temperature difference between the sample vessel and the thermometer-heater leads were enclosed in a single large sheath and inserted in an M-shaped holder at the base of the auxiliary shell. A very thin film of stopcock grease was used to improve the thermal contact. The thermometer and heater leads were also enclosed in the same sheath. Thus, the thermocouples sensed the temperature of the "thermometer-heater lead control" relative to that of the electrical leads at the sample vessel where the thermocouple sheath was in thermal contact. One of the "voltage taps" for the calorimeter vessel heater was located in the thermocouple sheath and the other at the "thermometer-heater lead control." (See fig. 1.)

2.5. Measurement Instruments and Procedures

2.5.1. Temperature Measurements

The platinum resistance thermometers (laboratory designations: 1057849 in the sample vessel and 1066759 in the "thermometer-heater lead control") used in the measurements were calibrated in accordance with the International Practical Temperature Scale of 1968 [12]. The temperatures in T given in this paper are equivalent to the International Practical Kelvin Temperature Scale expressed as T_{68} in reference [12].

The measurements of thermometer resistance were made to the nearest 0.00001Ω . Initially a manual Mueller bridge was used and later an automatic Mueller bridge. The resistance-time observations with the automatic Mueller bridge were obtained on punched cards and were analyzed by means of a computer to calculate the "initial" and "final" thermometer resistances associated with each experimental point. The observations with the manually operated bridge were processed by means of a desk calculator.

As mentioned previously in section 2, the thermometer calibration method was tested by intercomparing the temperature indications of the calibrated platinum resistance thermometers in the sample vessel and in the "thermometer-heater lead control." The calorimeter used in the measurements with beryllium nitride presented in this paper did not have the radiation shield for the "thermometer-heater lead control." (See sec. 2.3.2(b).) Hence, electric power

b. *Radiation shield for the "thermometer-heater lead control."* This shield was designed to be used only when the thermometer in the sample vessel is being calibrated relative to the reference thermometer installed in the "thermometer-heater lead control." During heat-capacity measurements no electric power is applied to the shield, i.e., the temperature of the shield is not controlled. When the thermometer is being calibrated, the shield and the "ring lead-control" are controlled to be at the same temperature as that of the "thermometer-heater lead control." Under such operating conditions no electric power is needed to maintain the "thermometer-heater lead control" at the same temperature as that of the sample vessel. As explained later, a more satisfactory thermometer calibration is achieved by avoiding the small fluctuations which would otherwise occur in the reference thermometer resistance with any change in the electrical power to the "thermometer-heater lead control." (See section 2.5.1.)

The radiation shield was a thin (0.810 mm thickness) copper cylinder with one end closed with a copper disk of the same thickness. The shield was gold plated and polished. There were no grooves on this shield.

The shield heater wire was wound helically, without overlapping, on the cylindrical portion of the shield using lacquer for cement. A flat heater was cemented on the flat end. The flat heater was prepared by spirally winding the heater wire, wet with lacquer, between two Teflon disks spaced at the thickness of the wire. The heater was removed from between the Teflon disks after drying and cemented to the shield.

2.3.3. Thermocouples

The number of constantan-Chromel-P thermocouple junctions in series between temperature control points was as follows:

- a. between "ring lead-control" and "thermometer-heater lead control": 3;
- b. between "thermometer-heater lead control" and sample vessel: 6;
- c. between sample vessel and its radiation shield: 4;
- d. between "thermometer-heater lead control" and its radiation shield: 3.

In addition to the above thermocouples, copper-constantan thermocouples were used to check the temperature of the "ring lead-control," the radiation shields, and the "thermometer-heater lead control" relative to that of the "tempering ring." To achieve temperature control the "tempering ring" was always colder than any of the other "points."

2.3.4. Temperature Control of the Adiabatic Shields

The temperatures of the "ring lead control," "thermometer-heater lead control," and the radiation shields were controlled by adjusting the electric current in the heater wires wound on them. An automatic control system combining electronic and electromechanical equipment was used in conjunction with the differential thermocouples to adjust the heater currents [11].

was introduced also during thermometer calibration into "thermometer-heater lead control" to maintain its temperature as close as possible to that of the sample vessel. Small temperature fluctuations (corresponding to about 0.2 or 0.5 mK) occurred in the "thermometer-heater lead control" from the control adjustments of the electric power, necessitating many rapid measurements to obtain a suitable average. The results of the "calibration" at a few selected temperatures are summarized in table 1. The maximum spread is 4 mK. The thermometer in the "thermometer-heater lead control" indicated more often higher temperatures than the thermometer in the sample vessel, but this deviation may be partially due to the difference in the temperature interpolation of the thermometers [9]. The degree of agreement in the temperature scale is satisfactory for heat-capacity measurements, particularly since the calibration data at many temperature points will be fitted by the method of least squares to equations in $R(T)$ and the temperature changes corresponding to the observed sample vessel thermometer resistances calculated from the equations.

TABLE 1. Comparison of the temperatures of platinum resistance thermometers in the calorimeter sample vessel and the "thermometer-heater lead control" under adiabatic control

Thermometer No. 1057849 in Calorimeter Sample Vessel	Thermometer No. 1066759 in "Thermometer-Heater Lead Control"	Temperature Difference No. 1057849-No. 1066759
T, K	T, K	mK
91.123	91.123	0
113.690	113.692	-2
137.255	137.258	-3
194.267	194.264	3
220.230	220.232	-2
251.932	251.930	2
267.055	267.059	-4
301.052	301.054	-2

In another calorimeter [21], identical in every respect to that used with beryllium nitride, a radiation shield was added around the "thermometer-heater lead control" to be used during thermometer calibration. When this radiation shield and the "ring lead-control" were controlled to be at the same temperature as that of the "thermometer-heater lead control," no electric power was needed to maintain the "thermometer-heater lead control" at the same temperature as that of the sample vessel. This added feature eliminated the small fluctuations in the "thermometer-heater lead control" that occurred with the control current adjustments. The calibration results obtained were comparable to those given in table 1, except that the measurements were more uniform and were obtainable more leisurely. Figure 1 shows the location of this auxiliary radiation shield and the calorimeter description given earlier in this paper includes this shield.

The calorimeter heater circuit employed was similar to that previously described [11]. The electrical energy, ΔQ , introduced into the calorimeter was determined from the product of the average calorimeter heater voltage, \bar{e} , the current, \bar{i} , and the time interval, τ , of electric power input:

$$\Delta Q = \bar{e}\bar{i}\tau. \quad (1)$$

The average \bar{e} and \bar{i} were obtained from a series of voltage observations made at equally spaced times during the heating period. A Wenner potentiometer in conjunction with a volt box, standard resistors, and saturated standard cells was used in the measurements. The standard resistors and the standard cells were calibrated at the National Bureau of Standards in terms of the national standards. A constant current supply, stable to about 2 parts per million (ppm), was the source of power for the calorimeter heater. By using the constant current supply in conjunction with the Ni-Cr alloy wire of low temperature-coefficient of resistance for the calorimeter heater, the heater voltage did not change during the heating period by more than 0.01 percent per minute over the entire temperature range of the heat-capacity measurements. Thus, the relatively slowly changing voltage was read quite conveniently, and with ease, to the five- to six-figure capability of the Wenner potentiometer.

The duration of each heating period τ was measured by means of a high-precision interval timer operated on the 60-Hz frequency standard provided at the National Bureau of Standards. The 60-Hz frequency standard is based on a 100-kHz quartz oscillator which is stable to 0.5 ppm. As a check, an electronic counter based on a thermostated 1-MHz quartz oscillator was used simultaneously in the measurement of the heating period. The electronic counter was checked periodically with a 100-kHz frequency standard wired into the laboratory. The estimated uncertainty in the determination of the heating interval was not greater than ± 0.01 s for any heating period, none of which was less than 2 min in these experiments.

3. Sample

The Be_3N_2 sample was specially prepared for the measurements by the Brush Beryllium Company, Cleveland, Ohio, by reacting pure nitrogen and beryllium powder at elevated temperatures and crushing the product to particle sizes between 20 and 50 mesh (0.8 and 0.3 mm sieve openings, respectively). The material received was thoroughly mixed in a controlled-atmosphere box containing dry argon (dew-point: -70°C) and samples were apportioned for chemical analysis, for the high-temperature relative enthalpy measurements [1], and for the low-temperature heat-capacity measurements described in this paper. The samples for the chemical analysis and the high-temperature enthalpy measurements were sealed in test tubes under dry argon. The sample that was poured into the low-temperature calorimeter

vessel weighed 97.415 g. The calorimeter vessel containing the sample was pumped at high vacuum and purged with dry helium gas several times and finally, helium gas at a pressure of 9300N/m² (70 torr) was sealed in the container with the sample.³ After completion of the measurements, the calorimeter vessel was opened in the controlled-atmosphere box and the sample was divided and sealed in polyethylene bags for chemical analysis. The sealed polyethylene bags were placed individually in screwcap jars which were in turn placed in desiccators, the whole operation being done in the controlled-atmosphere box.

The results of spectrochemical analysis of the sample obtained by the NBS Spectrochemical Analysis Section are summarized in table 2. Only the impurity elements that were detected are listed. The results of the chemical analyses on the material obtained by the Microchemical Analysis Section of the Bureau before and after the calorimetric measurements are given in table 3. For the nitrogen and total beryllium analyses, about 0.3-g samples were first dissolved in dilute hydrochloric acid and the solution diluted to 250 cm³ in a volumetric flask. A 10-cm³ aliquot was analyzed for nitrogen using the Kjeldahl method, the ammonia being titrated with 0.01 N hydrochloric acid that had been standardized against ammonium dihydrogen phosphate by means of the Kjeldahl procedure. The total beryllium was determined by precipitating the beryllium hydroxide in a 10-cm³ aliquot with ammonium hydroxide. The beryllium hydroxide was filtered, ignited, and weighed as BeO. The free beryllium was determined by dissolving 2-g samples in hydrochloric acid. The hydrogen formed was dried, converted to water, and weighed. No analysis was made for beryllium carbide, Be₂C. The analysis for free beryllium would include Be₂C, which forms methane and then water under the conditions of the analysis. The apparently low free beryllium analysis indicates very little Be₂C, if any.

TABLE 2. Summary of spectrochemical analysis of the sample of α -beryllium nitride, Be₃N₂—impurity elements that were detected

Element	Wt %	Element	Wt %
Al	0.001—0.01	Mg	0.001—0.01
Ca	<0.001	Mn	<0.001
Cr	0.001—0.01	Ni	0.001—0.01
Cu	<0.001	Si	0.01—0.1
Fe	0.01—0.1	Ti	0.001—0.01

Analysis by Elizabeth K. Hubbard, NBS Spectrochemical Analysis Section

The analysis for water represents all forms of hydrogen present in the sample. Samples (20 mg) were heated at 1050 °C in a carbon-hydrogen-nitrogen analyzer and the amount of water driven off was deter-

³The pressure was observed in mm Hg and converted to mm Hg at 0°C and standard gravitational acceleration of 980.665 cm/s² for the processing of the data. The conversion to N/m² was made using the definition: normal atmosphere = 101,325 N/m² = 760 torr (mm Hg at 0 °C and standard gravity)[13].

TABLE 3. Chemical analysis of the sample of α -beryllium nitride, Be₃N₂

Original Sample			
Element	wt %	Element	wt %
Be (total)	49.06	N	49.45
	49.09		49.52
			49.84
mean . . .	49.08	mean . . .	49.60
Be (free)	0.09	Cl	< 0.02
	0.11		
	0.09		
mean . . .	0.10	F	< 0.01
Sample Removed from Calorimeter Vessel			
Be (total)	48.72	N	48.97
	48.68		48.89
mean . . .	48.70	mean . . .	48.93
Be (free)	0.04	H ₂ O	1.16
	0.04		1.12
mean . . .	0.04	mean . . .	1.14
0	2.38 (average of 5 determinations)		

Chemical analysis by R. A. Paulson, NBS Microchemical Analysis Section

Oxygen analysis by activation method, S. Nargolwalla, NBS Activation Analysis Section

mined. The oxygen was determined by a nondestructive 14-Mev neutron activation technique. Five determinations were made using 6-g samples.

The results of the chemical analysis were found to be inconsistent and unexpected. The decrease in the free beryllium content in the samples before and after the measurements cannot be attributed to chemical reactions at temperatures of the measurements. (Small heat effects were observed above about 320 K. See later parts of this section for further details.) The difference is probably due to nonhomogeneity in the material, although relatively large samples (2 g) were used in this determination.

The decrease in the total beryllium content because of a chemical reaction during the heat measurements does not seem possible. If the observed heat effects resulted from a chemical reaction within the sample, the expected reaction would be:



This should lead to an increase in the apparent beryllium content, since the ammonia would be lost on opening the sample vessel.

For the material removed from the calorimeter

vessel after the heat measurements, the mass balance for beryllium found is not consistent in terms of the analyses obtained. The analyses for N, O, and total Be sum to 100.01 percent and the addition of H (0.13 percent) found as water makes the total weight percent 100.14. This is within the expected limits of accuracy of the chemical analyses. However, inconsistencies arise when these analyses are used to obtain mass balance among the chemical species that are expected to be present (Be_3N_2 , BeO , $\text{Be}(\text{OH})_2$, and Be metal). On the basis of the results of the oxygen and water analyses (2.38 and 1.14 percent, respectively), the percentage of beryllium as BeO and $\text{Be}(\text{OH})_2$ sums to 0.77 percent. When the Be metal (0.04 percent) and beryllium (47.22 percent) as Be_3N_2 , based on the nitrogen analysis, are added to 0.77 percent, the total beryllium becomes 48.03 percent. This is considerably lower than the total beryllium (48.70 percent) from the chemical analysis. The masses of the substances present also sum to considerably less than 100 percent (96.15% Be_3N_2 , 2.72% $\text{Be}(\text{OH})_2$, 0.56% BeO , and 0.04% Be metal; 99.47% total mass). These inconsistencies can be resolved if the Be metal analysis were higher (about 0.7 percent), but this is not possible since the estimated error in the chemical analysis for Be metal is much less than this value.

On the other hand, if the analysis shown in table 3 for water is ignored, the remaining analyses would become consistent on the basis that the substances present are only Be_3N_2 , BeO , and Be metal. All of the oxygen (2.38 percent) would then be taken to be present as BeO , which corresponds to 3.73 percent BeO or 1.34 percent Be. When the percentages of Be as Be_3N_2 and as Be metal are added to 1.34 percent, the total "calculated" Be is 48.61 percent. This is within the limits of chemical analysis found for total Be (48.70 percent). When the 96.15 percent Be_3N_2 , based on the nitrogen analysis, is added to the percentages of BeO and Be metal, the total weight percent is 99.92 percent. The analyses for total beryllium, nitrogen, and oxygen, as mentioned earlier, sum to 100.01 percent. These values are all within the limits of the chemical analysis.

The source of heat effects observed during the measurements (to be described later) can not be explained in terms of the known possible chemical reaction within the sample. The possible chemical reaction depicted by eq (2), in which the water from $\text{Be}(\text{OH})_2$ reacts with Be_3N_2 to form BeO and NH_3 , is not consistent with the chemical analyses. The reaction is obviously not possible if the water is securely held at the temperatures of the heat measurements. Duval and Duval [14] interpreted their thermal gravimetric analysis work to indicate that the decomposition of $\text{Be}(\text{OH})_2$ starts around 150 °C and that complete decomposition of $\text{Be}(\text{OH})_2$ to BeO and H_2O occurs only on heating to 951 °C. The observed loss in mass at temperatures below 150 °C was attributed to adsorbed water in their sample. If any moisture were present in the sample that was used in the work reported here, it was adsorbed between the times the sample was

removed from the furnace and received from the supplier.

After careful consideration of the various possibilities that could be selected on the basis of the chemical analyses and the estimated uncertainties that would arise from them, the choice was made to ignore the analysis obtained for water in the reduction of the heat-capacity measurements. The sample was taken to be 96.23 percent Be_3N_2 , 3.73 percent BeO , and 0.04 percent Be metal and corrections were applied to the observed values of heat capacity for BeO [15] and Be metal [16].

Two crystalline modifications of Be_3N_2 have been reported, the α - Be_3N_2 of bcc lattice with anti- Mn_2O_3 structure [17, 18] and the β - Be_3N_2 of hexagonal structure [18]. The α - Be_3N_2 transforms into the β - Be_3N_2 form at 1400 °C [18]. The x-ray examination by the NBS Crystallography Section of the sample after the heat-capacity measurements showed only the α - Be_3N_2 form within the limits of analysis of the method.

4. Results and Method of Data Reduction

Two series of measurements were made, one on the calorimeter vessel with sample (gross) and the other on the empty vessel (tare). Briefly, the measured energy increments (ΔQ) and the corresponding thermometer resistances (R) before and after heating for the two series of measurements were analyzed on the high-speed digital computer to obtain dQ/dR of the sample as a function of the thermometer resistance [19]. After adjusting for the helium exchange gas used with the Be_3N_2 sample, the values of heat capacity (dQ/dT) of the sample were then calculated at even temperatures from the dR/dT and the R - T calibration for the thermometer using the relation:

$$dQ/dT = (dQ/dR)(dR/dT). \quad (3)$$

In greater detail, the analysis procedure was to obtain first the best polynomial equation of the form

$$dQ/dR = \sum a_n R^n \quad (4)$$

to represent the experimental data on the empty calorimeter vessel (tare) [20]. The polynomial equation for tare measurements was then evaluated at the thermometer resistances observed for the gross measurements in order to obtain the energy increments for sample only (net) from the observations on the calorimeter vessel plus sample experiments, i.e.,

$$\Delta Q_R(\text{sample}) = \Delta Q_R(\text{gross}) - \Delta Q_R(\text{tare}). \quad (5)$$

(Hereafter, $\Delta Q_R(\text{sample})$ will also be referred to as observed data on the sample and the corresponding quantity $\Delta Q/\Delta T(\text{sample})$ as observed sample heat capacity). The best polynomial equation giving dQ/dR for the sample only was then obtained and dQ/dT calculated according to eq (3) above.

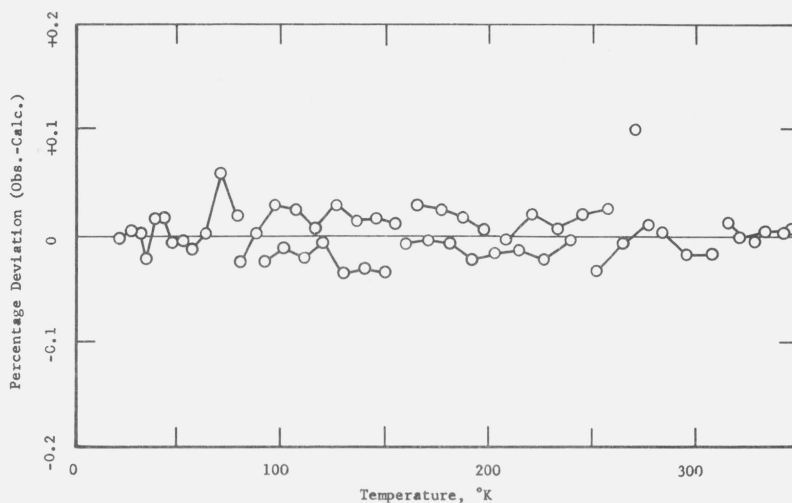


FIGURE 4. Percentage deviation of the empty sample vessel heat capacities from the polynomial equation:

$$dQ/dR = \sum_{n=-4}^{+10} a_n R^n.$$

Consecutive measurements obtained during the day are connected by lines.

Figure 4 shows the deviation of the experimental data on the empty container from corresponding values calculated from the polynomial equation fitted by the method of least squares to the energy-resistance observations. The range of the polynomial was from $n = -4$ to $n = +10$ (see eq (4)). The root-mean-square (rms) of the percentage deviation of all data from the polynomial equation was 0.02 percent. For the final reduction of the data the two poor points shown in figure 4 were not considered; the rms of the percentage deviation of the remaining data was 0.008 percent.

Due to increasingly poorer precision at the lowest experimental temperatures the sample data were fitted with two overlapping equations. Figure 5 shows the deviation of the sample data from the polynomial (n ranging from 0 to 4) fitted to the data over the temperature range 20 to 110 K and figure 6 the deviation of the data from the polynomial (n ranging from -2 to $+10$) fitted over the temperature range 60 to 315 K. Heat capacity values calculated from the two equations agreed within 0.02 percent over the temperature range 80 to 100 K. The heat capacity values obtained from the two equations were joined at 90 K. The rms of the percentage deviation of the observed sample heat capacity from the polynomial equations is 0.06 percent above 50 K. The deviation increases below 50 K.

Figures 5 and 6 show the precision of the gross measurements; the boundary curves represent the effect on the final smooth values of a change of 0.025 percent in the values of the heat-capacity measurements for the empty and filled sample vessel; e.g., at 100 K (fig. 6), a change in the heat capacity of 0.025 percent of the empty vessel causes slightly less than 0.1 percent change on the sample while a similar change of the gross measurements causes about 0.12 percent change on the sample. Figures 5 and 6 show

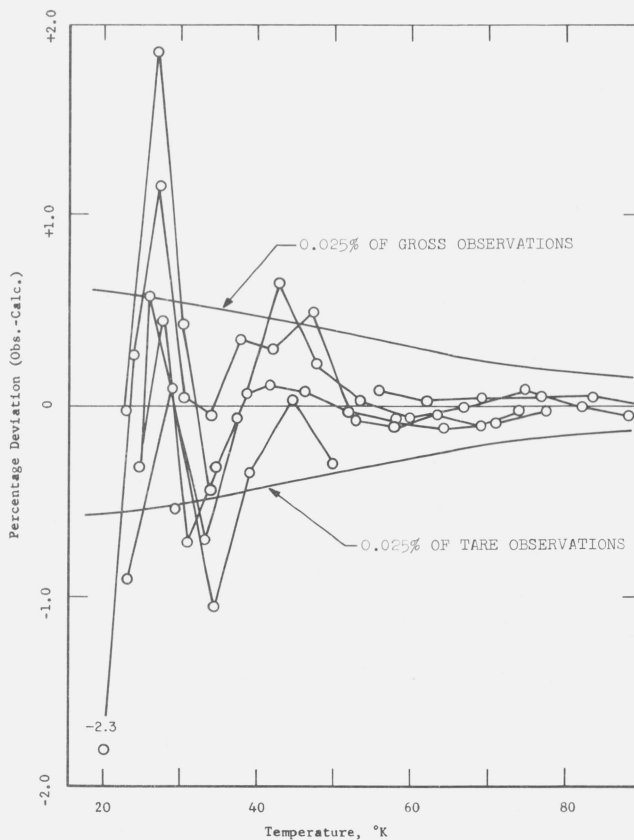


FIGURE 5. Percentage deviation of the α -beryllium nitride sample heat capacities from the polynomial equation:

$$dQ/dR = \sum_{n=0}^{+4} a_n R^n.$$

Consecutive measurements obtained during the day are connected by lines.

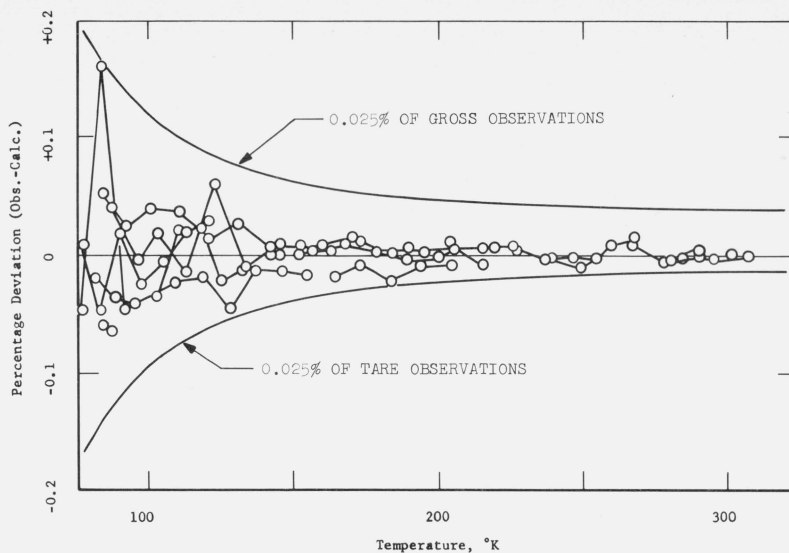


FIGURE 6. Percentage deviation of the α -beryllium nitride sample heat capacities from the polynomial equation:

$$dQ/dR = \sum_{n=-2}^{+10} a_n R^n.$$

Consecutive measurements obtained during the day are connected by lines.

that above 50 K the precision of the gross measurements is about ± 0.01 percent.

As mentioned earlier, heat effects were observed during the measurements of the heat capacity above about 320 K. The final results that are presented are based on the data obtained between 20 and 315 K subsequent to heating above 320 K. In figure 7 are shown values of heat capacity initially obtained between 80 and 315 K prior to heating above 320 K.

The base line (zero line) of the figure corresponds to the final smoothed values. Above 150 K, the values of the initial measurements and those after heating above 320 K are shown to be essentially the same. Below 150 K, the values of the initial measurements are somewhat higher. Since no data were obtained initially below 80 K, no comparison could be made below 80 K between the values before and after heating above 320 K. In the range 80 to 315 K, however,

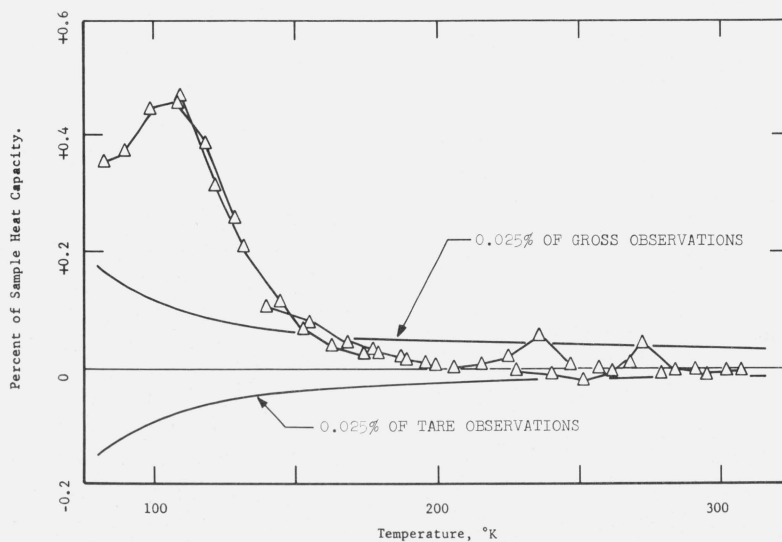


FIGURE 7. Percentage deviation of initial measurements from the final selected α -beryllium nitride sample heat capacities.

Consecutive measurements obtained during the day are connected by lines.

the heating above 320 K did not make a large change in the heat capacity of the sample, at the most about 0.5 percent at 100 K. The comparison shows that the heat capacity of the sample was not affected grossly when heated above 320 K.

The values of heat capacity of Be_3N_2 that were generated at evenly spaced temperatures from dQ/dR in accordance with eq (2) were corrected for BeO [15] and Be metal [16] and converted to molal basis. The molecular weight was taken to be 55.05 g, based on the 1961 atomic weight scale [22]. These molal values were analyzed further for extrapolation to 0 K. The final selected values below 20 K are based on the extrapolation of the experimental heat capacity using the heat-capacity function:

$$C = 1943.73(705/T)^{-3} \quad (6)$$

J/K·mol.

The final smoothed values of heat capacity have a relatively large uncertainty arising from the possible impurities in the sample. Above 100 K the estimated uncertainty is 0.5 percent and below this temperature 1 percent.⁴

The values of heat capacity from 0 to 315 K were applied in the usual thermodynamic relations:

$$H_T - H_0^c = \int_0^T C dT, \quad (7)$$

$$S_T = \int_0^T (C/T) dT, \quad (8)$$

and

$$G_T - H_0^c = (H_T - H_0^c) - TS_T, \quad (9)$$

to obtain the thermodynamic properties. The values are given in table 4.

⁴The uncertainty, as used with the values obtained in this paper and indicated by the symbol \pm , is an estimate reached by examining contributions to the inaccuracy from imprecision and possible systematic errors in the measurements. The authors estimate that there is a 50-50 chance that the error is no larger than that indicated.

Justice [3] recently reported heat-capacity measurements on $\alpha\text{-Be}_3\text{N}_2$ of 96.7 percent purity. The significant impurities were BeO-2.7 percent, Be metal-0.2 percent, C-0.1 percent, and Fe-0.3 percent. The entropy at 298.15 K that Justice [3] reported is 8.170 cal/K·mol, which is in good agreement with that (8.23 ± 0.08 cal/K·mol) found in this investigation. The values of heat capacity obtained also join satisfactorily, in both the magnitude of heat capacity and its slope, with those derived from the high-temperature relative enthalpy measurements reported by Douglas and Payne [1]. (See Douglas and Payne [1] for tables of thermodynamic properties of Be_3N_2 up to 1200 K).

The results presented in this paper (figs. 5, 6, and 7) show that the precision obtained on the empty vessel is ± 0.01 percent over the entire temperature range of the measurements, while on the vessel with sample the precision is ± 0.01 only above about 50 K. There is no explanation for the precision of the gross measurements to be poorer than that of the tare measurements at the lower temperatures. A large part of the apparently poorer precision of the sample data at the lower temperatures is believed to be caused by the poorer fit of the equation to the sample data. The trends in the deviations shown in figure 5 partially support this belief. A part of the poorer equational fit to the sample data may be caused by the choice of the equation to represent the tare data, resulting in a complex net sample data to be fit by an equation. A high-quality fit of the gross data is also not easily achieved because of the combined contribution of the sample and vessel. Because of the poor quality of the beryllium nitride sample, an intensive experimental study of these questions was considered inadvisable. Also, the uncertainty at these lower temperature contributes very little to the overall uncertainty in S_{298} . Therefore, no further experimental measurements were made on beryllium nitride. The study of these "finer details" is planned when an opportunity arises on a material of high purity.

TABLE 4. Molal thermodynamic functions for α -beryllium nitride, (Be_3N_2), solid phase

Gram Molecular weight = 55.0500 g

Cal = 4.1840 J

$T, \text{K} = 273.15 + t \text{ } ^\circ\text{C}$

T	C_p^c	$(H_T^c - H_0^c)$	$(H_T^c - H_0^c)/T$	$(S_T^c - S_0^c)$	$-(G_T^c - H_0^c)$	$-(G_T^c - H_0^c)/T$
K	J/K	J	J/K	J/K	J	J/K
0.00	0.0000	0.0000	0.00000	0.00000	0.00000	0.00000
5.00	.0007	.0009	.00017	.00023	.00029	.00006
10.00	.0055	.0139	.00139	.00185	.00462	.00046
15.00	.0187	.0702	.00468	.00624	.0234	.00156
20.00	.0444	.222	.0111	.0148	.0740	.00370
25.00	.0863	.541	.0217	.0289	.181	.00722
30.00	.147	1.116	.0372	.0497	.374	.0125
35.00	.230	2.048	.0585	.0782	.690	.0197
40.00	.339	3.459	.0865	.116	1.171	.0293
45.00	.480	5.492	.122	.163	1.865	.0414

TABLE 4. Molal thermodynamic functions for α -beryllium nitride, (Be_3N_2) , solid phase—Continued

Gram Molecular weight = 55.0500 g

Cal = 4.1840 J

$$T, \text{K} = 273.15 + t \text{ } ^\circ\text{C}$$

T	C_p°	$(H_T^\circ - H_0^\circ)$	$(H_T^\circ - H_0^\circ)/T$	$(S_T^\circ - S_0^\circ)$	$-(G_T^\circ - H_0^\circ)$	$-(G_T^\circ - H_0^\circ)/T$
K	J/K	J	J/K	J/K	J	J/K
50.00	.660	8.323	.166	.223	2.826	.0565
55.00	.888	12.170	.221	.296	4.117	.0749
60.00	1.172	17.294	.288	.385	5.813	.0969
65.00	1.522	24.000	.369	.492	7.999	.123
70.00	1.944	32.634	.466	.620	10.771	.154
75.00	2.446	43.575	.581	.771	14.238	.190
80.00	3.029	57.226	.715	.947	18.521	.232
85.00	3.697	74.005	.871	1.150	23.752	.279
90.00	4.451	94.338	1.048	1.382	30.070	.334
95.00	5.292	118.66	1.249	1.645	37.626	.396
100.00	6.218	147.40	1.474	1.940	46.574	.466
105.00	7.227	180.98	1.724	2.267	57.078	.544
110.00	8.314	219.80	1.998	2.628	69.302	.630
115.00	9.473	264.24	2.298	3.023	83.416	.725
120.00	10.701	314.65	2.622	3.452	99.590	.830
125.00	11.993	371.35	2.971	3.915	117.99	.944
130.00	13.343	434.67	3.344	4.411	138.79	1.068
135.00	14.747	504.87	3.740	4.941	162.16	1.201
140.00	16.201	582.23	4.159	5.503	188.26	1.345
145.00	17.699	666.96	4.600	6.098	217.25	1.498
150.00	19.236	759.28	5.062	6.724	249.29	1.662
155.00	20.807	859.37	5.544	7.380	284.54	1.836
160.00	22.406	967.40	6.046	8.066	323.14	2.020
165.00	24.030	1083.5	6.567	8.780	365.24	2.214
170.00	25.671	1207.7	7.104	9.522	410.99	2.418
175.00	27.326	1340.2	7.658	10.290	460.51	2.631
180.00	28.990	1481.0	8.228	11.083	513.93	2.855
185.00	30.659	1630.1	8.811	11.900	571.37	3.089
190.00	32.328	1787.6	9.408	12.740	632.96	3.331
195.00	33.994	1953.4	10.017	13.601	698.81	3.584
200.00	35.655	2127.5	10.638	14.483	769.01	3.845
205.00	37.307	2309.9	11.268	15.383	843.67	4.115
210.00	38.949	2500.6	11.907	16.302	922.87	4.395
215.00	40.579	2699.4	12.555	17.238	1006.7	4.682
220.00	42.195	2906.3	13.211	18.189	1095.3	4.979
225.00	43.796	3121.3	13.873	19.155	1188.6	5.283
230.00	45.381	3344.3	14.540	20.135	1286.9	5.595
235.00	46.948	3575.1	15.213	21.128	1390.0	5.915
240.00	48.496	3813.7	15.890	22.133	1498.2	6.242
245.00	50.024	4060.0	16.572	23.148	1611.4	6.577
250.00	51.531	4313.9	17.256	24.174	1729.7	6.919
255.00	53.015	4575.3	17.942	25.209	1853.1	7.267
260.00	54.475	4844.0	18.631	26.253	1981.8	7.622
265.00	55.911	5120.0	19.321	27.304	2115.7	7.984
270.00	57.321	5403.1	20.011	28.363	2254.8	8.351
273.15	58.197	5585.0	20.447	29.033	2345.2	8.586
275.00	58.707	5693.2	20.702	29.427	2399.3	8.725
280.00	60.067	5990.1	21.393	30.497	2549.1	9.104
285.00	61.404	6293.8	22.084	31.572	2704.3	9.489
290.00	62.717	6604.1	22.773	32.652	2864.8	9.879
295.00	64.008	6920.9	23.461	33.735	3030.8	10.274
298.15	64.811	7123.8	23.893	34.419	3138.1	10.525
300.00	65.278	7244.2	24.147	34.821	3202.2	10.674
305.00	66.522	7573.7	24.832	35.910	3379.0	11.079
310.00	67.735	7909.3	25.514	37.002	3561.3	11.488
315.00	68.905	8251.0	26.194	38.095	3749.0	11.902

H_0° and S_0° apply to the reference state of the solid at 0 K.

5. References

- [1] Douglas, T. B., and Payne, W. H., *J. Res. Nat. Bur. Stand. (U.S.)*, **73A** (Phys. and Chem.), 471 (1969).
- [2] Satoh, S., *Sci. Papers Inst. Phys. Chem. Research (Tokyo)* **34**, 888 (1938).
- [3] Justice, B. H., *J. Chem. Eng. Data* **14**, 384 (1969).
- [4] Scott, R. B., Meyers, C. H., Rands, R. D., Jr., Brickwedde, F. G., and Bekkedahl, N., *J. Res. Nat. Bur. Stand. (U.S.)*, **35**, 39 (1945), RP1661.
- [5] Furukawa, G. T., Reilly, M. L., and Piccirelli, J. H., *J. Res. Nat. Bur. Stand. (U.S.)*, **68A** (Phys. and Chem.), 381 (1964).
- [6] Furukawa, G. T., Reilly, M. L., and Piccirelli, J. H., *J. Res. Nat. Bur. Stand. (U.S.)*, **68A** (Phys. and Chem.), 651 (1964).
- [7] Furukawa, G. T., and Saba, W. G., *J. Res. Nat. Bur. Stand. (U.S.)*, **69A** (Phys. and Chem.), 13 (1965).
- [8] Furukawa, G. T., and Saba, W. G., *J. Res. Nat. Bur. Stand. (U.S.)*, **71A** (Phys. and Chem.), 3 (1967).
- [9] Hoge, H. J., and Brickwedde, F. G., *J. Res. Nat. Bur. Stand. (U.S.)*, **28**, 217 (1942) RP1454.
- [10] Furukawa, G. T., Reilly, M. L., and Saba, W. G., *Rev. Sci. Instr.* **35**, 113 (1964).
- [11] Westrum, E. F., Jr., Furukawa, G. T., and McCullough, J. P., Adiabatic low-temperature calorimetry, in *Experimental Thermodynamics, Calorimetry of Non-Reacting Systems*, Vol. 1, pp. 133-214 (Butterworths, London, 1968).
- [12] The International Practical Temperature Scale of 1968, adopted by the Comité International des Poids et Mesures, *Metrologia* **5**, 35 (1969).
- [13] United States Department of Commerce, *Nat. Bur. Stand. (U.S.)*, Handb. 102, ASTM Metric Practice Guide (1967) 46 pp.
- [14] Duval, T., and Duval, C., *Anal. Chim. Acta* **2**, 53 (1948).
- [15] Furukawa, G. T., and Reilly, M. L., unpublished measurements on BeO.
- [16] Furukawa, G. T., and Reilly, M. L., unreported results of analysis of literature heat-capacity data on beryllium metal.
- [17] Stackelberg, M. V., and Paulus, R., *Z. physik. Chem.* **22B**, 305 (1933).
- [18] Eckerlin, P., and Rabenau, A., *Z. anorg. allgem. Chem.* **304**, 218 (1960).
- [19] Furukawa, G. T., and Reilly, M. L., *J. Res. Nat. Bur. Stand. (U.S.)*, **69A** (Phys. and Chem.) 5 (1965).
- [20] Walsh, P., *Comm. ACM* **5**, 511 (1962).
- [21] Furukawa, G. T., Saba, W. G., and Ford, J. C., *J. Res. Nat. Bur. Stand. (U.S.)*, **74A** (Phys. and Chem.), No. 5, 631-639. (Sept.-Oct. 1970).
- [22] Cameron, A. E., and Wichers, E., *J. Am. Chem. Soc.* **84**, 4175 (1962).

(Paper 74A5-625)